CHAPTER 2

BASIC PRINCIPLE

2.1 Corundum

2.1.1 Corundum and their coloration

Natural corundum of pure Al_2O_3 structure is clear or has no color, thus its several different colors usually depend upon the allochromatic which is one or more of the transition elements. The various colors of corundum are unpredictable properties which can be described by many coloration mechanisms. Furthermore, the color of corundum has about 150 tones, but the naked-eye can identify only 31 tones. Corundum is called according to the color attributes which is tone, saturation, principal and secondary hue, respectively, e.g. medium dull white sapphire (Themelis, 1992). The causes of colors can be summarized as the followings.

i) Transition metal impurities (Allochromatic)

For transition–metal elements (3d and 4d valence electrons), crystal field theory is used to describe the influence of ligand around the metal (Burns, 1993). According to ligand field theory, corundum is the octahedral field and molecular orbital electron configuration can also be illustrated by this theory. Each of energy level of compound varies which depends upon the crystallography field. As shown in Figure 2.1, Cr^{3+} has 3d orbital valence electron which can substitute Al^{3+}. This leads

to octahedral field as shown in red color. According to ligand field theory (Miessler and Tarr, 2003), the metal ion interacts with a ligand which assumed as a point charge by electrostatic force only. Later, a ligand would split those energy levels which depend on a valence state of metal and ligand. By this way, the electrons of a transition element are repelled from the ligands which can occupy the d-orbitals at the farthest end from the direction of approach to the ligands (Atkins *et al.,* 2010). The valence electron of Cr^{3+} will interact with the six point charges of oxygen located around them. These electrons have 3d–orbital, spliting to the five degeneracy wavefunctions, some of them lie along the axis (i.e. $d_{X^2-Y^2}$, d_{Z^2}) will be destabilized more than the orbitals which lie among the axis (i.e. d_{XY}, d_{YZ}, d_{XZ}) (Vincent, 2001). As shown in Figure 2.2, Tanabe-Sugano relation shows the relation plot between electron energy level splitting versus the crystal field energy (Ueda and Tanabe, 2010). Each line in the relation refers to the energy level satisfied to the spectroscopic notation. The crystal field energy of any matter is vary depend upon many factor such as atomic radius, lattice spacing, etc., for example the different of crystal field energy in glass (SiO_2) and alumina (Al_2O_3) are illustrated in this figure. Remind that the spectroscopic notation as seen in Appendix A. These energy levels can occupy the allowed or forbidden of the absorption and the fluorescence of corundum as shown in Figure 2.3. The schematic (a) to (d) in this figure show the allowed process of electron transition either absorption or fluorescence between the energy levels. This phenomena associate with the absorption (ABS.) or transmission (TRNSM.) of any color in the ruby (Lehmann and Harder, 1970). In other words, the red appearance in a ruby is produced by the transmission of a red color. Furthermore, the yellow color is

similarly produced as the above description, but the substitution ion is Fe^{3+} (Spinolo *et al.*, 2009).

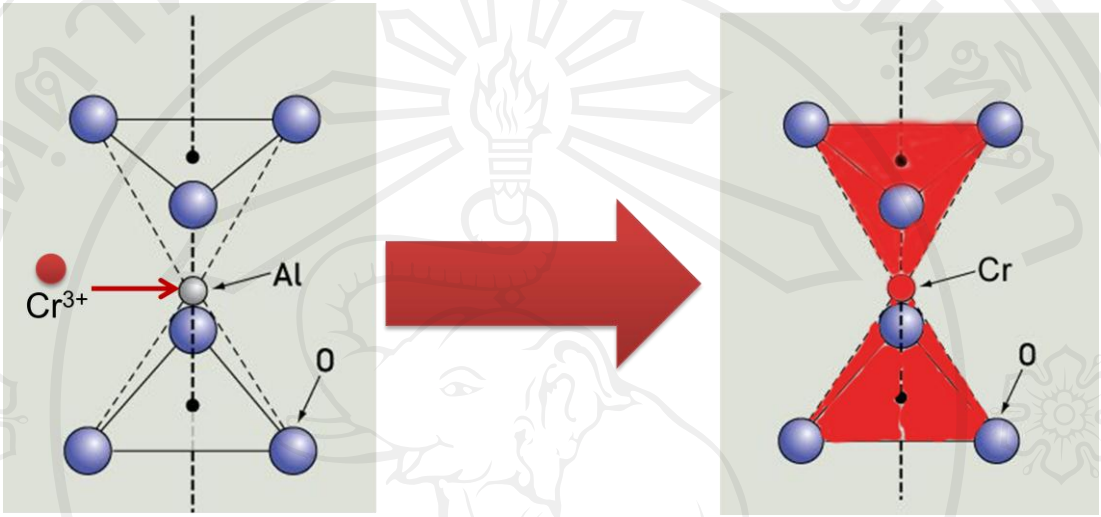

Figure 2.1. The red color appearance of corundum is happened from the substitution of Al^{3+} by Cr^{3+}.

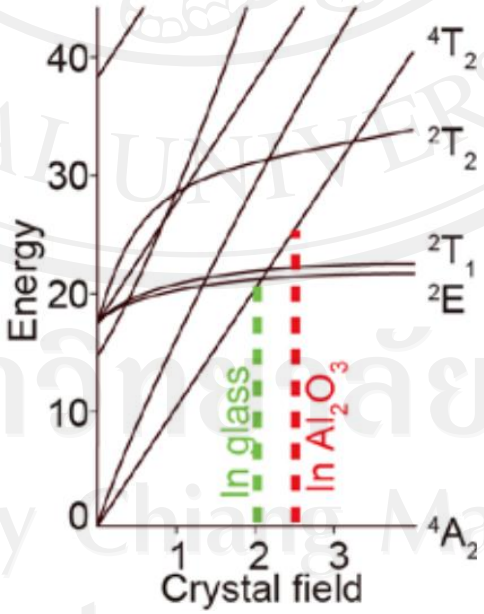

Figure 2.2. Tanabe-Sugano relation for 3d-orbital electrons (Ueda and Tanabe, 2010).

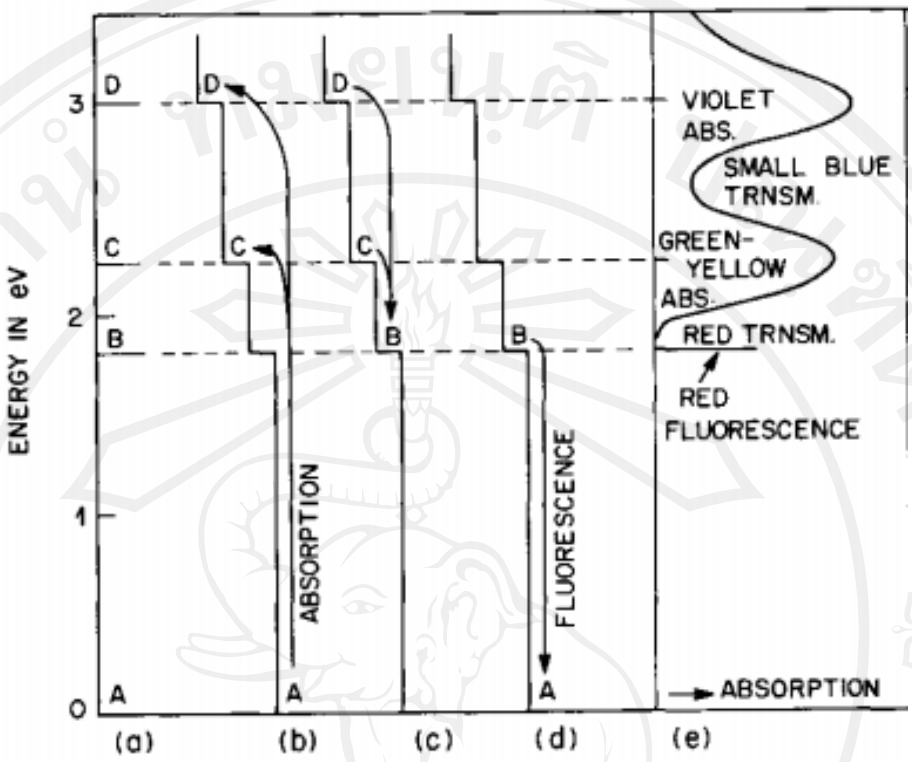

Figure 2.3. The energy level diagram, transition, and color absorption/fluorescence mechanisms in a ruby (Nassau, 1978).

ii) Intervalence charge transfer (IVCT) process

As mentioned earlier that corundum is the octahedral structure field, the valence electrons of the ion can exchange between the molecules by absorption of a photon. The molecular orbital formalism describes the situation where electrons are not simply established on single ions as in the crystal field formalism (Nassau, 2001). This formalism is similar to the crystal field formalism which has the electron transition process and link to the transition opportunities. For corundum case, the metal-metal charge transfer is the major source of blue coloration, i.e. Fe^{2+}/Ti^{4+} as

shown the alteration in Equation 2.1 demonstrates the intervalence charge transfer process between the two ions.

$$Fe^{2+} \rightarrow Fe^{3+} + e^{-}, \qquad Ti^{4+} + e^{-} \rightarrow Ti^{3+} \tag{2.1}$$

An electron of Fe^{2+} may transfer to Ti^{4+} by absorption of the photon energy, and vice versa. As a result, the broad peak is occurred about 560 nm and resulting in the well-known of deep blue color. The dichroism is observed which is caused by the distance from Fe to Ti is 2.65 Å in the optic axis (C-axis), and 2.79 Å in the perpendicular direction. The ratio of Fe^{2+} to Ti^{4+} refers to the intense of blue color, i.e. the lack of Ti^{4+} let the sapphire become colorless. Another charge transfer process occurring for Fe such as Fe^{2+}/Fe^{3+} and Fe^{3+}/Fe^{3+} as shown in Equation 2.2 – 2.3, respectively. The former gives the deep blue color and the latter can also produce the yellowish color.

$$Fe^{2+} \rightarrow Fe^{3+} + e^{-}, \qquad Fe^{3+} + e^{-} \rightarrow Fe^{2+} \tag{2.2}$$

$$Fe^{3+} \rightarrow Fe^{3+} + e^{-}, \qquad Fe^{4+} + e^{-} \rightarrow Fe^{3+} \tag{2.3}$$

iii) Metals: Energy band theory

Pure corundum which contains only the Al_2O_3 has energy gap about 5.4 eV (equivalent to 229.76 nm electromagnetic wave), so it becomes colorless appearance. In other words, the electron in valence band cannot jump up to conduction band because of the insufficient of the visible light energy region.

iv) Color center: Irradiation process

When the energetic ions collide on the target atom, a vacancy of lattice atom can be produced by the sputtering phenomenon, e.g., F center, F^+ center, etc. Consequently, the evidence of this process is the luminescent broad peak which can be observed by the IL technique.

2.1.2 The corundum deposit

There are two main types of corundum deposits, primary and secondary. Each of these can be classified, based on geological activities as shown in Figure 2.4, into metamorphic deposits and basaltic (magmatic) deposits (Atichart *et al.*, 2010). Magma, the hot fluid flowing in the earth's mantle contains many elements, mainly are iron and aluminum. Sometimes magma can erupt to the Earth's outer crust and cool down to form basaltic rock. During the cooling down process, corundum or aluminium oxide may form as a crystalline structure in the rock. Almost all trace elements in the magma are recrystallized and combined into an alumina structure. Thus, this deposit type is termed "basaltic" or "magmatic" which this corundum type is rich in iron. The other deposit type, metamorphic, occurs when magma has thermal contact with a neighboring rock, which is heated, deformed and recrystallized into a new structure. Therefore, corundum of these deposits occasionally have a high content of Ti and low of Fe (Read, 2005). The dominant elements in each of deposit are occurred by the different mechanism which described in Figure 2.5. Previous studies have reported that the population field appearance of trace element concentration can indicate a corundum's origin (Sun *et al.*, 2001; Osipowicz *et al.*, 1995).

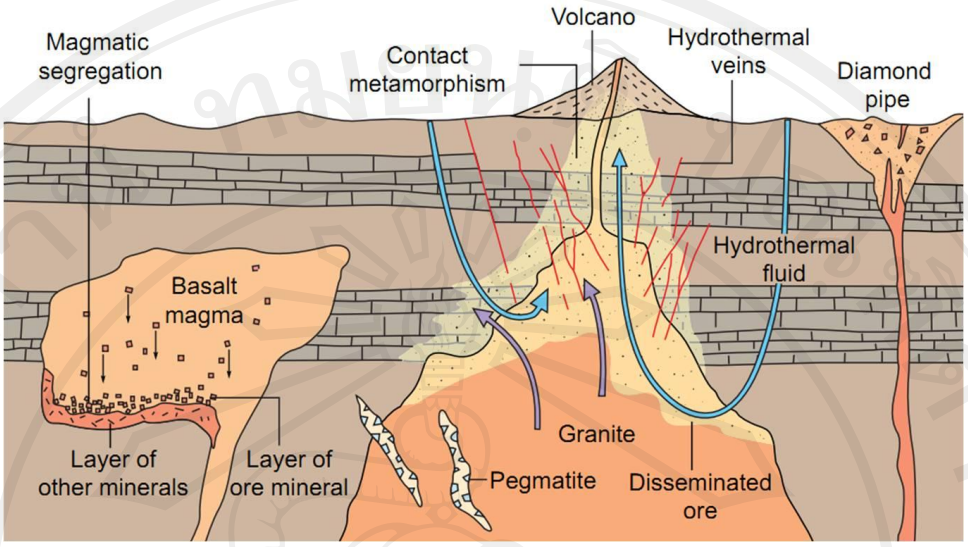

Figure 2.4. The sub-crust activity of the earth (Hamblin *et al.*, 2000).

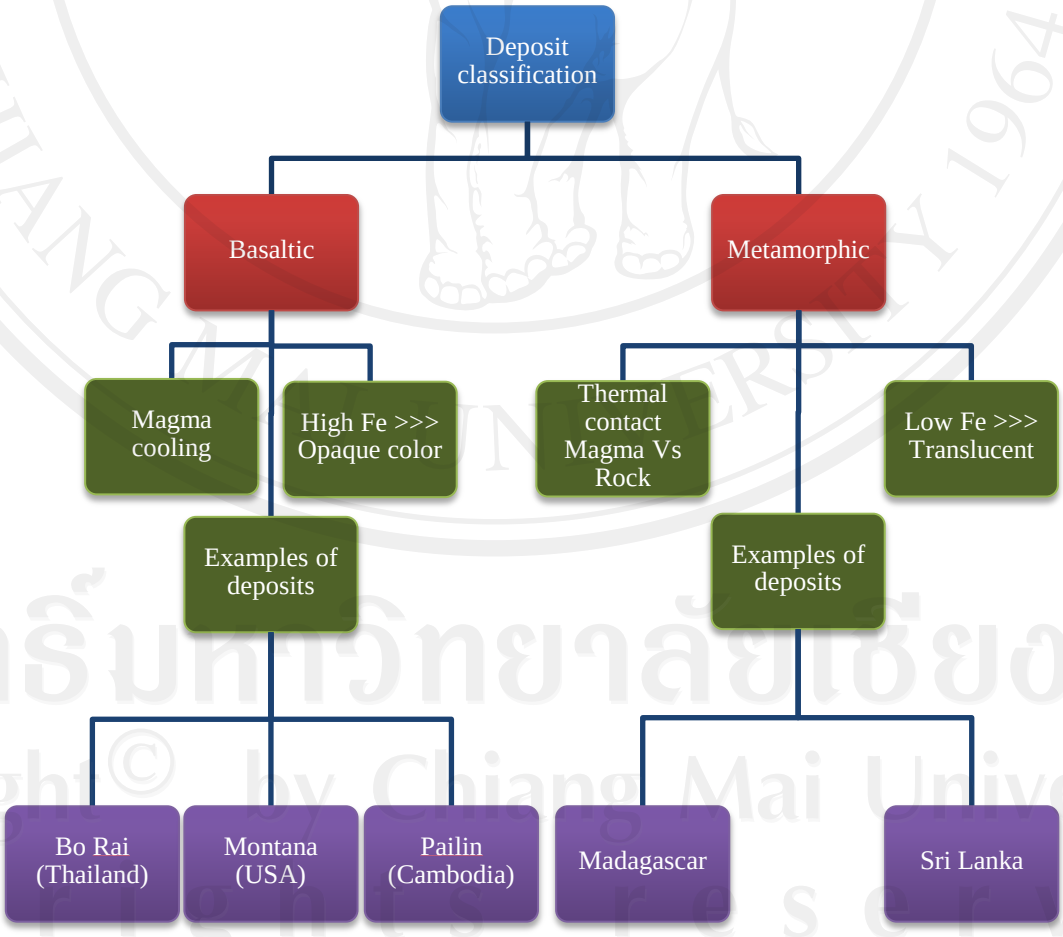

Figure 2.5. The predominant of basaltic and metamorphic deposits of corundum.

2.1.3 Color enhancement of corundum

In present day, corundum becomes an alternative jewelry because of its many good physical and chemical qualities. Gem traders always enhance them by various treatments in order to upgrade the physical property which related to the value. Nevertheless, the conventional methods such as heat treatment or irradiation method, consume very long time for the alteration, and unaccepted by some consumer or organization. The heat treatment technique needs electrical furnace that can feed any gas into the furnace chamber during treatment. This process can be distinguished into two main conditions, i.e. reducing, and oxidizing which would be chosen according to the type of corundum. The different condition can be identified by the oxygen content in the furnace during the heat treatment (Themelis, 1992). In case of lacking of oxygen concentration, called as the reduce condition, this condition usually use to enrich the light blue sapphire to be more intense in blue or eliminate the yellowish (brownish) tint in the green sapphire. On the other hand, the richness of oxygen, i.e. oxidizing condition, can intensify green color to be a yellowish tone, eliminate the violet tint, etc. Furthermore, the diffusion of some ion is added in some conditions to activate the modification; mainly is a Be-diffusion which invented by the Thai trader (Limsuwan *et al.*, 2008). The description for above alteration is the exchange of different states of the valence electron in corundum that depends upon the surrounding concentration (Kitbutrawat, 2006). The isovalent ion (existing valence state equal to Al^{3+}) can exchange dramatically with the matter, however, the rapidity of the reaction is influenced by the mass, energy, and direction of that diffusion process. By this way, the overall time consuming is more than days or months. Another method is irradiation process, this technique usually modify with the gem

which has the color by the color center mechanism such as tourmaline, quartz (Chanthaphun, 2008). The gems are placed in the radioactivity shielding box with gamma ray isotopic source. The energetic photons can induce color center in corundum which can produce a variety of color related to the surroundings atoms.

2.2 Ion implantation for gemstone modification

2.2.1 Basic knowledge of ion-solid interaction

A low energy incident ion mostly interacts with the nucleus of the target's atom called of "nuclear collision" (Averback, 2010). This phenomenon is dominantly appearing in the low energy ion or low atomic number element. Energetic ion which is accelerated by electrostatic field keeps on original chemical property whereas the gain of enormous kinetic energy. As shown in Figure 2.6, only the collision process is focused on the losing of energy of incident ion by random collision with the target nuclei. The collision process can divide into two types, elastic collision and inelastic collisions, which are different by the conservation of kinetic energy for the former and the opposite for the latter collision process as summarized from Carter and Colligon (1968). The former allows the incident ion to reflect back and the reflected ion has cascade collision with another target nuclei until its energy is less than the binding energy of atom in the lattice. Secondly, the incident ion can penetrate the surface of the target sample and has cascade mechanism in the previous situation. While the collision process occurs, the following phenomena can happen:

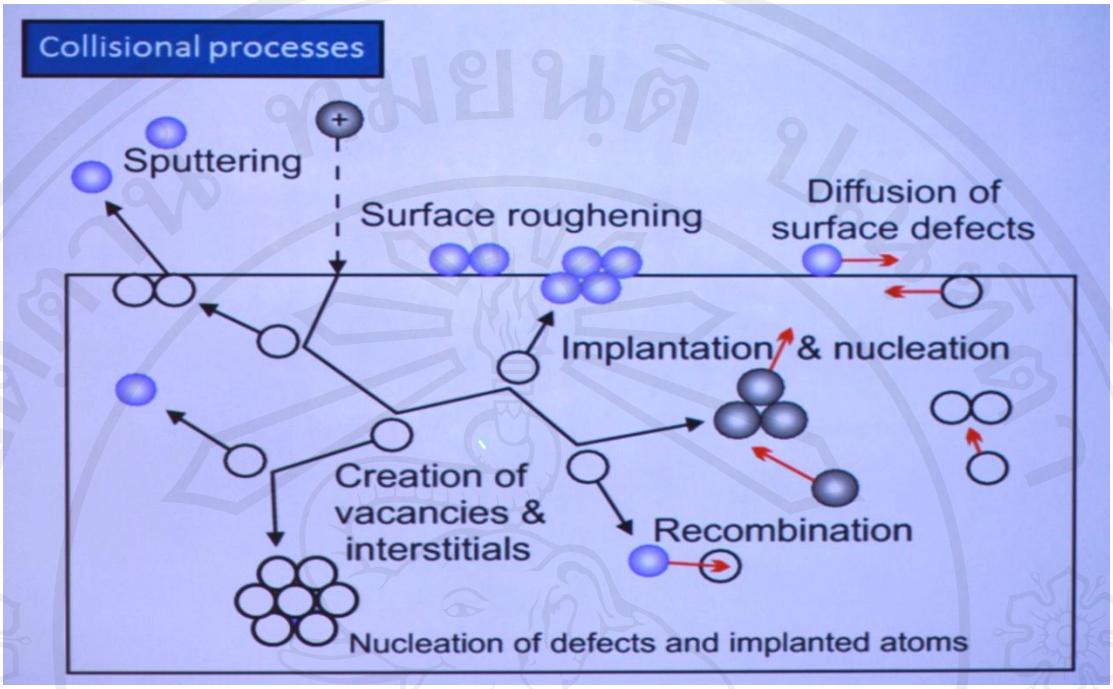

Figure 2.6. The incident ion induces several phenomena in the matter (Facsko, 2012).

1) Sputtered atom is the loosely bound atom of the target sample.
2) Secondary electron is the excited electron caused by the collision.
3) Electromagnetic wave or photon is produced by the transition of electron in the outer shell by the excitation process.
4) Electromagnetic wave or photon is produced by the transition of electron in the inner shell by the ionization process.
5) Auger electron is the escape electron caused by the photon in 3) – 4).

Accordingly, as long as the trajectory of the ion in the matter, the loss of kinetic energy would dissipate to electron cluster around the target atom. The kinetic energy of incident ion can transform to another energy form such as heat, photon, phonon, etc. The relation between the energy loss of incident ion and penetration

distance in the sample is called a "linear stopping power ($\frac{dE}{dx}$) or specific energy" which is related as seen in Equations 2.4 – 2.5 (Profio, 1979):

$$\frac{dE}{dx} = \rho N_A \left(\frac{Z_T}{W_T} \right) (Z_I e^2)^2 f(E_I, m_I) \qquad (2.4)$$

where, $f(E_I, m_I) = \left(\frac{2\pi}{E_I} \cdot \frac{m_I}{m_e} \right) \ln \left[\frac{4 m_e E_I}{m_e I} \right]$

E_I = incident ion's energy = $\frac{1}{2} m_I v_I^2$

m_I = incident ion's mass

v_I = incident ion's velocity

e = electron charge

m_e = electron mass

Z_T = atomic number of target atom

Z_I = atomic number of incident ion

I = average activated energy for excitation (Turner, 1995)

$$I = \begin{cases} 19.0 \text{ eV} & Z_T = 1 \\ 11.2 + 11.7 Z_T \text{ eV} & 2 \le Z_T \le 13 \\ 52.8 + 8.71 Z_T \text{ eV} & Z_T = 1 \end{cases} \qquad (2.5)$$

The straight distance that the incident ion can penetrate till stop is called of the "projected range" which differ in each of ion type and energy as shown in Figure 2.7. The energy loss among this range was also described by the "Stopping cross-section" (Yu, 1997).

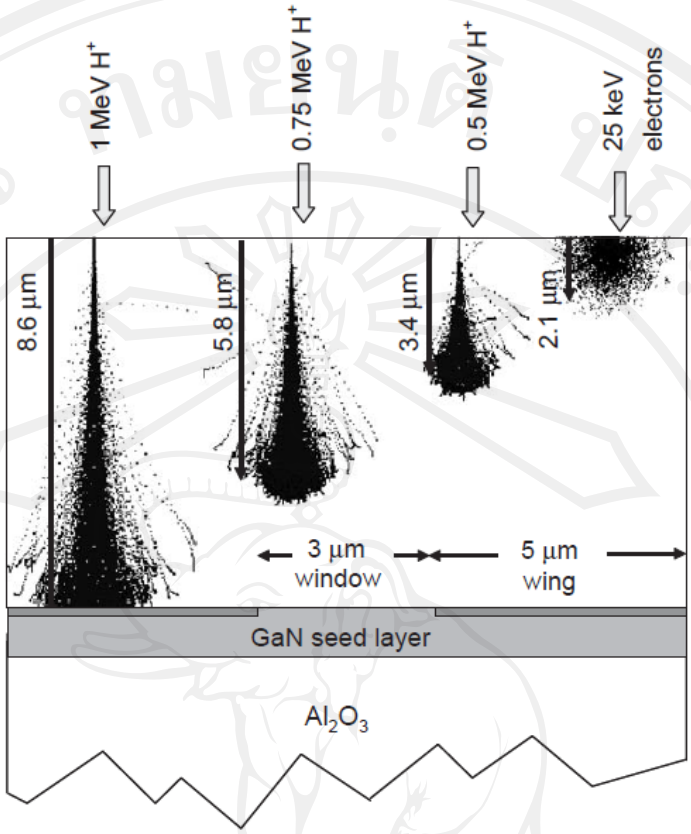

Figure 2.7. The different types of ion track in GaN (Teo *et al.*, 2004).

Over decades, the ion implantation is one of the keys of the materials modification due to its highly precise potential in controlling the implantation process and flexibility for various materials types. The ion implantation can specify the condition precisely, affect the whole matter or selective area, and enhance mechanical, chemical, electrical, or optical properties of materials. It has generally been applied in an industry but rarely in a gem business. One of the interesting experiment is the sapphire or ruby modification by using the ion implantation for the semiconductor improvement. However, the enhancement is only applied for synthetic corundum for the semiconductor or laser industry (Townsend *et al.*, 1994, Aoki *et al.*, 1996, Moroño and Hodgson, 1997, Ueda and Tanabe, 2010).

2.2.2 Ion implanter

More than decades, the ion beam techniques were applied in the materials modification work. Ion implantation which is performed by the ion implanter, is used for various surface modification. The machine is used for ion acceleration by the electric field. This treatment can enhance the physical, chemical, optical, or electrical properties of the solid matter. By this way, the ions alter the element location of the sample which also causes much chemical and physical change in the target by transferring their energy and momentum to the electrons or atomic nucleus of the target. This causes a crystal structure change in the target which can be damaged or destroyed by the energetic collision phenomenon as mentioned earlier. Since the ions have higher momentum, they can knock the target atoms out of their places in the crystal structure with more effective than the electron beam. The ion implanter consists of four main parts including ion source, ion analyzing system, accelerator section, scanning system (if any), and beam focusing system.

i) Nitrogen and argon ions beam implantation

Positive ions of either nitrogen molecules or argon atoms was generated from a Freeman type ion source of a 200 kV Varian ion implanter as shown in Figures 2.8 (a) – (b). There are an analyzing magnet for selecting ion species and energy, and beam scanning system for uniformly increasing the irradiation area. The total ion beam energy is the sum of an extraction voltage at the ion source and an acceleration voltage of the accelerating tube. During operation, the implanter is maintained at high voltage, thus the surrounding must be dry, cool, and allows only for technical officer. The working temperature and humidity of the room should be below 25 ^{o}C and 40%,

respectively, for preventing the heating up and moisture breakdown. Accompanied with the above, the basic concept and operating process are described by Labphu (2002).

Figure 2.8. (a) The photo of Varian Ion Implanter of Chiang Mai University.

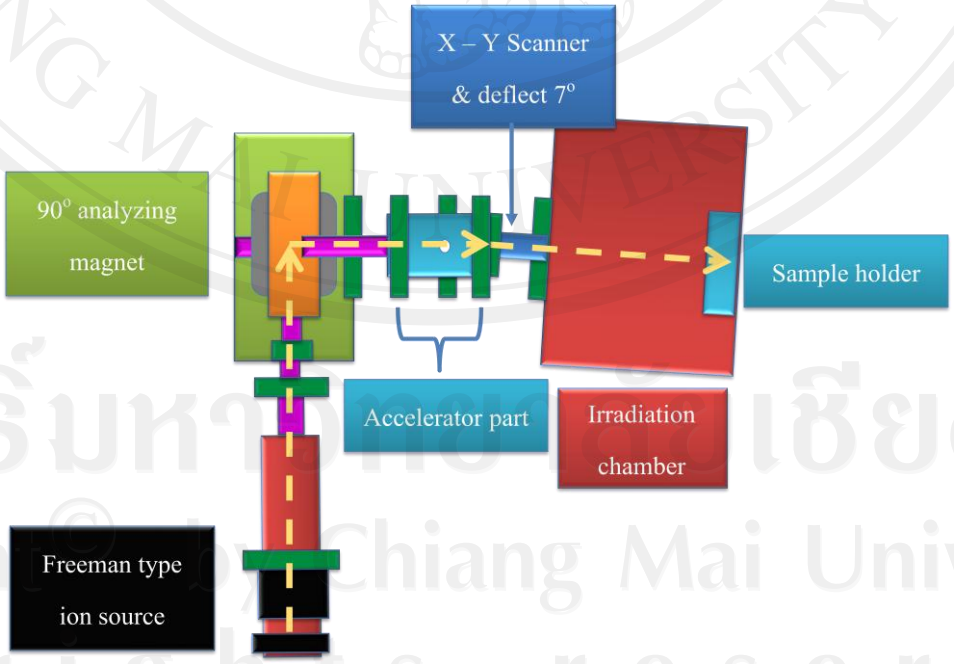

Figure 2.8. (b) The schematic diagram of Varian Ion Implanter.

Consequently, the electrical scanning plates can produce a rectangular cross section beam with 10x10 cm^2 size. Furthermore, the ion beam is deflected clockwise about 7 degree from the original direction, as shown in Figure 2.9, for removing neutral particles. Accompanied with, the measurement of the ion current at the four corner using the four-Faraday cup for adjusting the uniform distribution of the ion beam. Foregoing, the remaining ion beam was collimated to circular cross section with radius about 10 cm-diameter to a target section. Each of corundum would be attached on the sample holder by a piece of double-sided carbon tape, as shown in Fig 2.10. The sample holder was set up at the end of chamber and the driving motor can rotate it to be in perpendicular with the beam direction as shown in Figure 2.10. At the center of the sample holder, there is a hole of ~10 mm diameter which connects with a Faraday cup on the back of the sample holder. This Faraday cup, used for the fluence monitoring during operation, has the cross-sectional area about 0.64 times smaller than the hole in the middle of the sample holder.

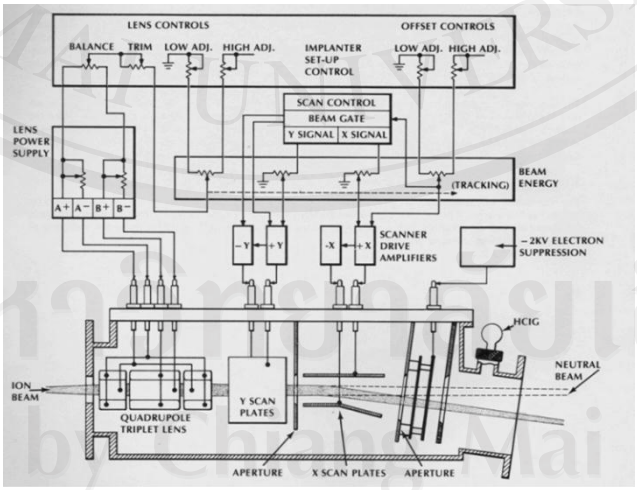

Figure 2.9. The schematic diagram of the focusing, scanning, and deflecting systems of the implanter (Varian/Extrion Division, 1980).

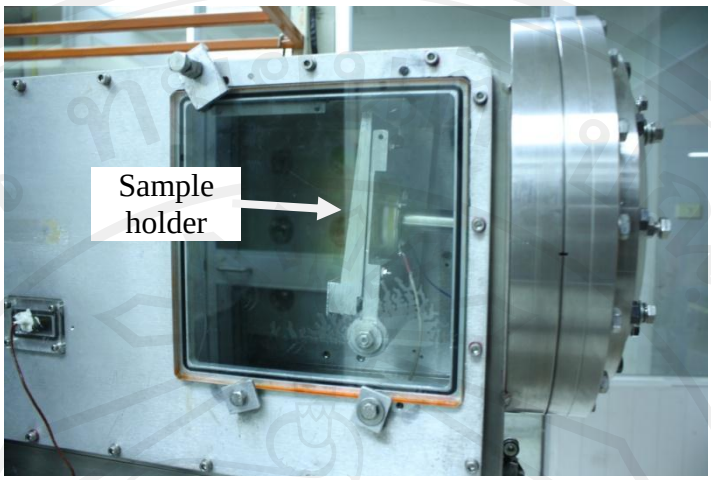

Figure 2.10. The sample holder at the end of beamline.

ii) Oxygen ion beam implantation

The negative ion beam was produced by a cesium sputter ion source. The irradiation system, as shown in Figure 2.11, consists of the ion source, the focusing system, the mass analysis system, and the irradiation chamber. In this case, the MnO_2 powder is used to produce the O^- ions. The oxygen negative ions left the ion source with kinetic energy of 23 keV. The electrostatic steerer and Einzel lens were used to control the beam quality for focusing the horizontal and vertical beam direction. Finally, an analyzing mass magnet is used to select the required ions. The ion beam was about 1 – 2 cm diameter at irradiation chamber. Each of corundum was attached to the fan-like sample holder. This holder has nine leaves which could be turned around to match up with the ion beam direction. For ion beam current measurement, the Faraday cup with 2 cm diameter is placed in front of the target system which could be inserted to intercept the beam before and after irradiation process. The negative oxygen beam current was very high because of its ionization energy, so the

ion current at this section is about 20 – 30 μA depending on the ion source parameters adjustment. By the way, the fluence was considered to vary in this experiment which could be calculated by the below calculation.

Let, "Q" is total charge per ion (C)

"N" is number of ion (ion)

"e" is electric charge of electron (C)

"I" is ion current at the target (A)

"t" is ion impact time (s)

"A" is ion beam cross section area (cm^2)

"D" is the ion beam fluence calculation

From,

$$Q = \int Idt$$

Thus,

$$Ne = \int Idt$$

Divided by "A" thoroughly,

$$D = \frac{N}{A} = \frac{\int Idt}{eA}$$

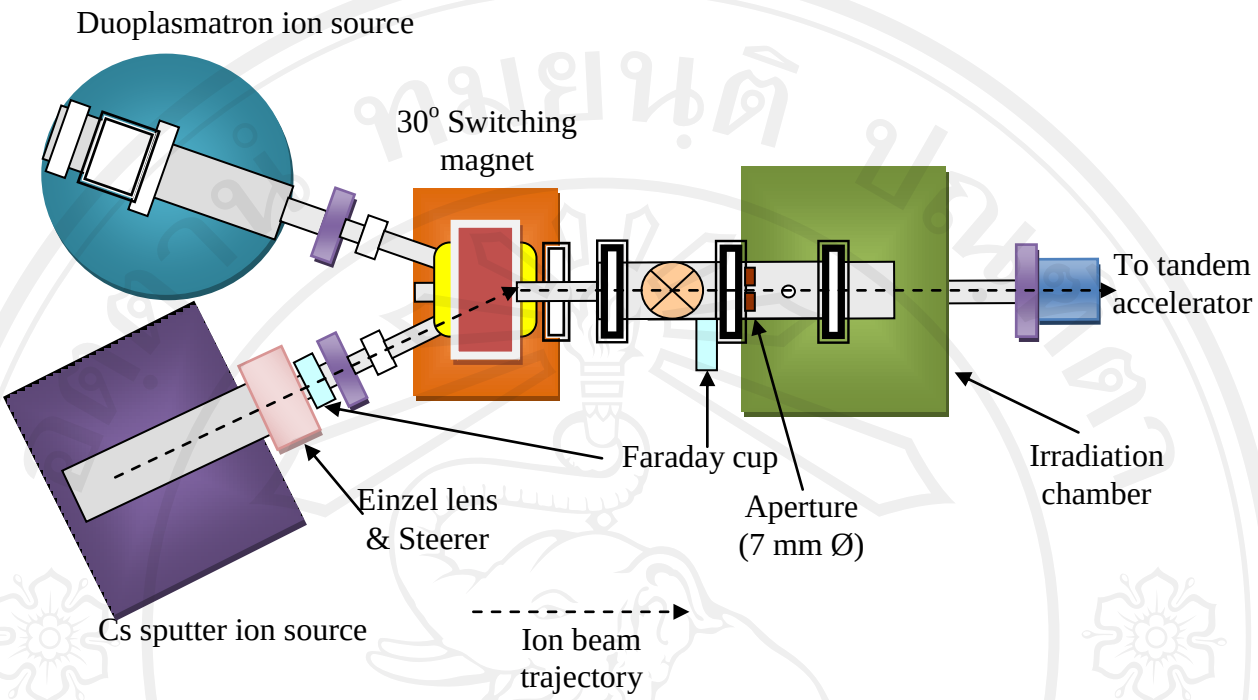

Figure 2.11. The diagram of the O^- ions irradiation system.

2.3 Ion beam analysis (IBA)

Ion beam analysis (IBA) used in this study were particle-induced X-ray emission (PIXE) and ionoluminescence (IL). The 2 MeV proton beams were produced by the 1.7 MV tandem accelerator of Chiang Mai University as shown in Figure 2.12. Only key principles of the two analytical techniques are described here. More details can be found elsewhere (Kamwanna, 2008).

2.3.1 Particle-induced X-ray emission (PIXE)

Particle-induced X-ray emission (PIXE) is quite similar to energy dispersive X-ray spectroscopy (EDS) in the scanning electron microscope which measure the characteristic X-ray emission from the sample atom. The principal difference is the

stimulated particle which EDS uses electron beam while PIXE uses proton beam. As a result, PIXE is superior over EDS in an accurate penetration depth adjustment and a lot of bremsstralung X-ray background. The background radiation is produced by the three main causes as follows. The first one is the kinetic energy of the incident proton lose to the target atom, therefore, this process leads to eject the electron in sample atom. These electrons are decelerated by the collision and produce the continuous X-ray so called of a secondary electron bremsstrahlung (SEB) appearing as a broad band at low energy region. Although this effect screens the low characteristic X-ray energy, there is count rate less than the technique which use electron as the incident ion such as EDS. The next situation is the decelerating of the incident proton by the target atom

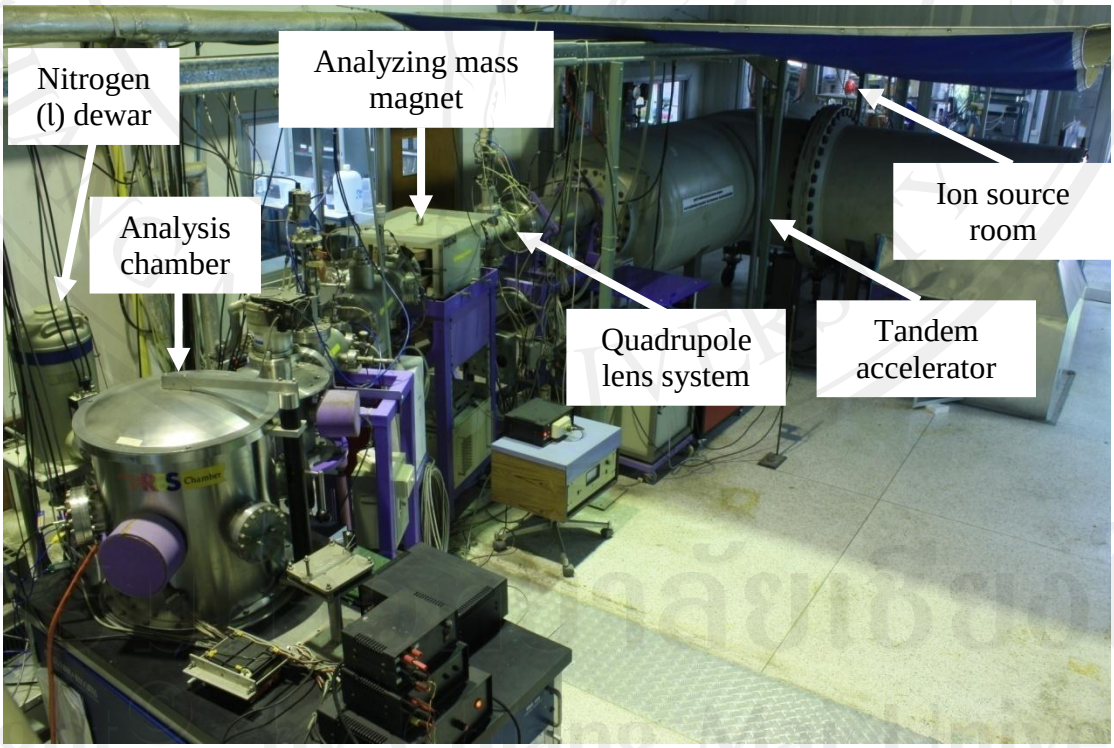

Figure 2.12. The 1.7 MV tandem "Tandetron" accelerator of Chiang Mai University with analysis chamber at the end of the beamline.

, as a result, the continuous background is occurred in every region of the X-ray energy acquisition which occurs dramatically with the enormous ion current. Eventually, an insulator sample such as corundum has the charging-up effect on the surface by the accumulation of incident protons, so an electron cluster produced by the electron shower is applied to reduce the bremsstrahlung effect. The characteristic X-ray is generated by the incident ion collides with the inner shell electrons, then, the vacancy is generated at this energy level. Later, the outer shell electron can transit to fill the vacancy followed by the selection rules (Kamwanna, 2008):

$$\Delta n \geq 1,\ \Delta l = \pm 1,\ \text{and}\ \Delta j = \pm 1,\ 0$$

where, n is the principal quantum number

l is the angular momentum number

j is the total angular momentum number

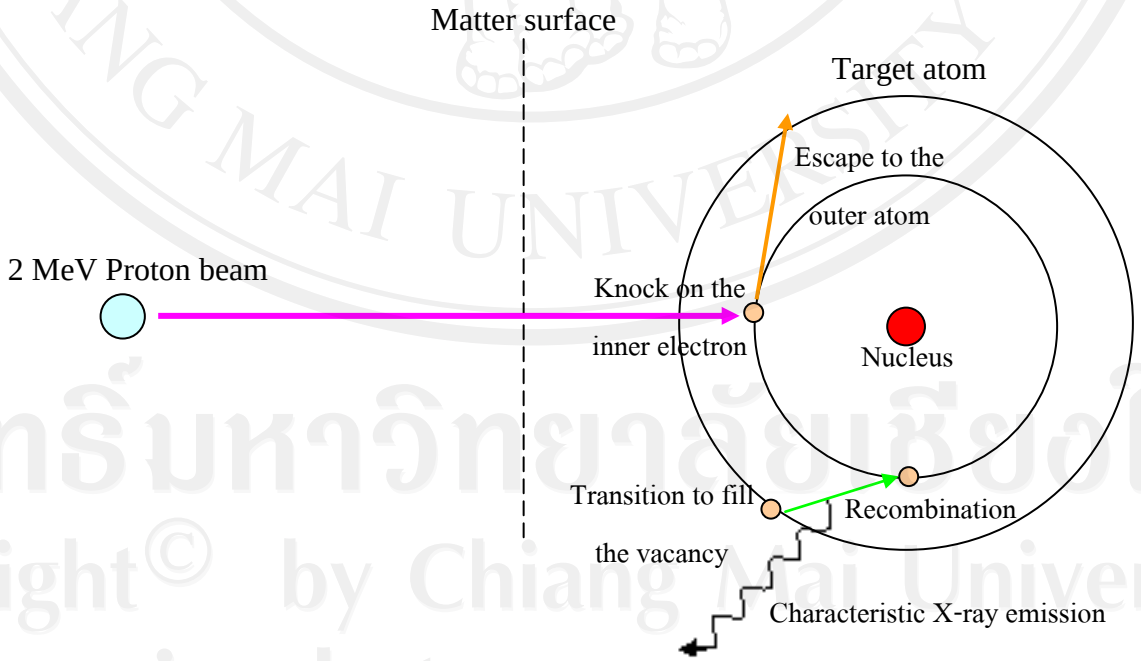

Figure 2.13. The diagram of the characteristic X-ray production process.

Although, these electrons are attracted by the high coulomb potential about keV, the energetic incident proton has sufficient energy to excite these electrons. Eventually, the transition of electron process releases the precise excess energy in the form of characteristic X-rays, as shown in Figure 2.13. The transition process is the radiation of spontaneous emission which the X-ray energy corresponds to the difference of electron binding energies between the two levels.

2.3.2 Ionoluminescence (IL)

While the energetic ion is colliding with a sample, it induces many effects. One of these is a vibration transition mode which occurs between vibrational levels. It is well known that some material shows a sign of luminescence. This can be classified to two main types, e.g., fluorescence and phosphorescence. Ionoluminescence (IL) likewise is potentially a highly sensitive method for measuring optically active impurities and defects in samples. There are some difference between IL and other luminescence techniques that energetic ion is used for exciting of the sample, so it is possible to reach higher electronic levels and can travel any depth by varying incident energy of the projectile. Not only the energetic protons impel to releasing tightly bound electron in crystal structure, but also stimulate the sharing of valence electrons in each atoms of molecule. It is well-known when these electrons are excited and recombine to the ground state which can emit a unique photon energy radiation. An amount of energy relates to the different of the transition energy in which maintain in visible light region as shown in Figure 2.14. IL is usually used complementarily to PIXE that gives information about a valence electron and their crystal form. As mechanism of IL occurs in molecular frontier, via distortion molecular energy state, it really complicate to

explain or extract data related to the optical properties. Just a little of research has been concentrated in this field; the mechanisms responsible for luminescence on sample radiation have yet to be studied thoroughly. Description of IL requires knowledge on luminescence mechanism of the whole molecular system of the investigated sample. However, both PIXE and IL were accustomed for research related to the origins, fingerprints qualities and trace elements quantities of gemstones.

This mechanism is occurred by the impurity in the crystal structure which has a few part per million by weight, but can be dramatically induced a strong luminescence by the high energetic ion. The light direction is random which depend upon the sample structure.

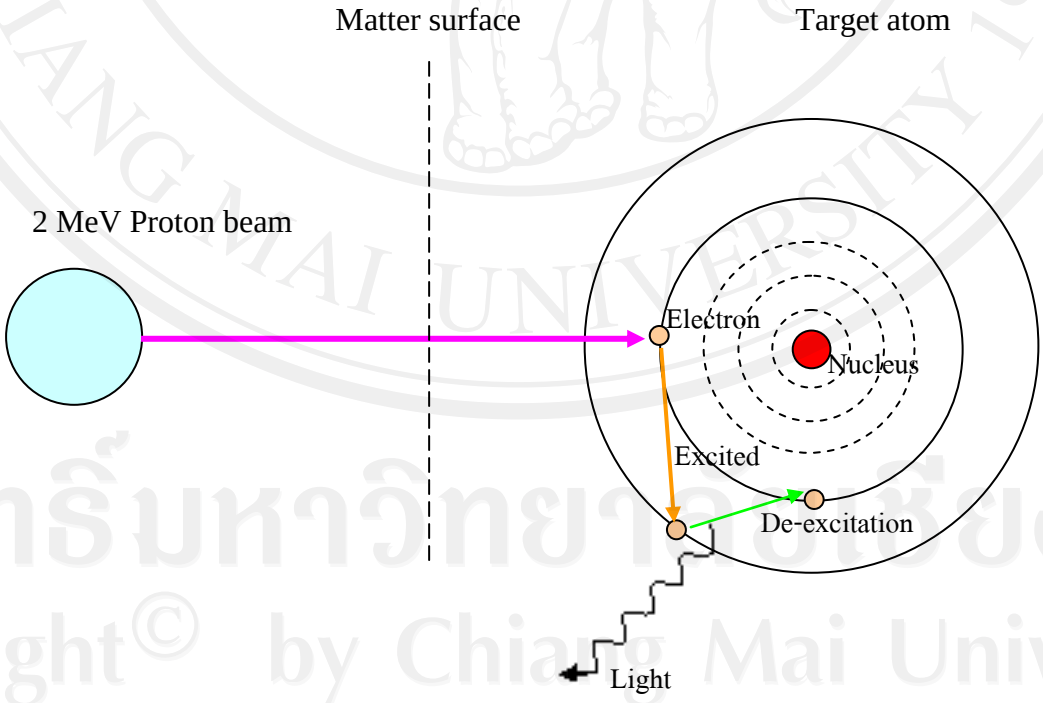

Figure 2.14. The diagram of the ionoluminescence process.

i) Transition metal (Lever, 1968)

The electron configuration of transition element is in the $3d^{(1-9)}$ form which causes the outer shell electron to strongly interact with the ligand as described by crystal field theory. Thus, the energy level of free electron in these ions split and has the interval depend upon the potential. In other words, the luminescence of transition element dramatically depends on the ligand surrounding the ion or different crystal structure. For example:

Cr^{3+} in corundum (Al_2O_3) produces red color luminescence at 694 nm

Mn^{2+} in witherite (Zn_2SiO_4) produces green color luminescence at 524 nm

Fe^{3+} in calcite ($CaCO_3$) produces orange color luminescence at 610 nm

Ti^{4+} in magnesite ($MgCO_3$) produces red color luminescence at 654 nm

Nonetheless, the characteristic of emission spectrum may be shifted by the considered of crystal structure and Stokes shift effect in crystal field.

ii) Rare earth elements (REEs)

The electron configuration of REEs is in the $4f^n[5s^25p^6]$ form which causes the 4f-orbital electron to strongly luminescence by electronic crystal field screening. The screening effect is caused by the 5s and 5p, so the energy levels of electron in REEs do not interact with crystal field. In other words, any REEs in different crystal structure always irradiate the luminescence as same as another. For instance, Pr^{3+} in zircon ($ZrSiO_4$) is luminescence at 485, 613, and 638 nm.

2.3.3 Data accumulation, acquisition and analysis of PIXE technique

Inside the analysis chamber is included with the Si(Li) detector, sample holder, electron gun, stepping motor, and beam slit. The sample holder connects to the four-set stepping motors, controlled by the a visual basic software, which can move the holder in the horizontal, vertical, tilt, and rotating direction to the appropriate position with the ion beam direction. Eventually, the Faraday cup which attaches with the sample holder at the end of the beamline for measuring the ion current at the target. The turbo pump is used for maintaining the vacuum state in the chamber as shown in Figure 2.15.

During measurement, 2 MeV energetic proton beams were collimated about 1 mm diameter slit which collide and penetrate into corundum at a depth of ~25 μm calculated by SRIM code (Zeigler *et al.*, 2008), and convince X-ray emissions. The Si(Li) detector (lithium – drifted silicon detector), set up at 120^{o} to the beam direction is used to detect X-rays at 87 mm from the sample. The detector is covered by the beryllium window with 25 μm thickness and used bias voltage of -500 volts (Somsorn, 2008).

This detector can effectively measure the X-ray in range of 1 – 20 keV, in case the more energy detection needs the more detector (semiconductor) thickness. The detector is coupled with a preamplifier (Canberra model 2008B) which connected to an amplifier (Canberra AFT Research Amplifier model 2025), and the MCA card (Maestro model A65-B32) in a personal computer at the control room. The accumulated data is analyzed by the GUPIXWIN software (Campbell and Maxwell, 2005)

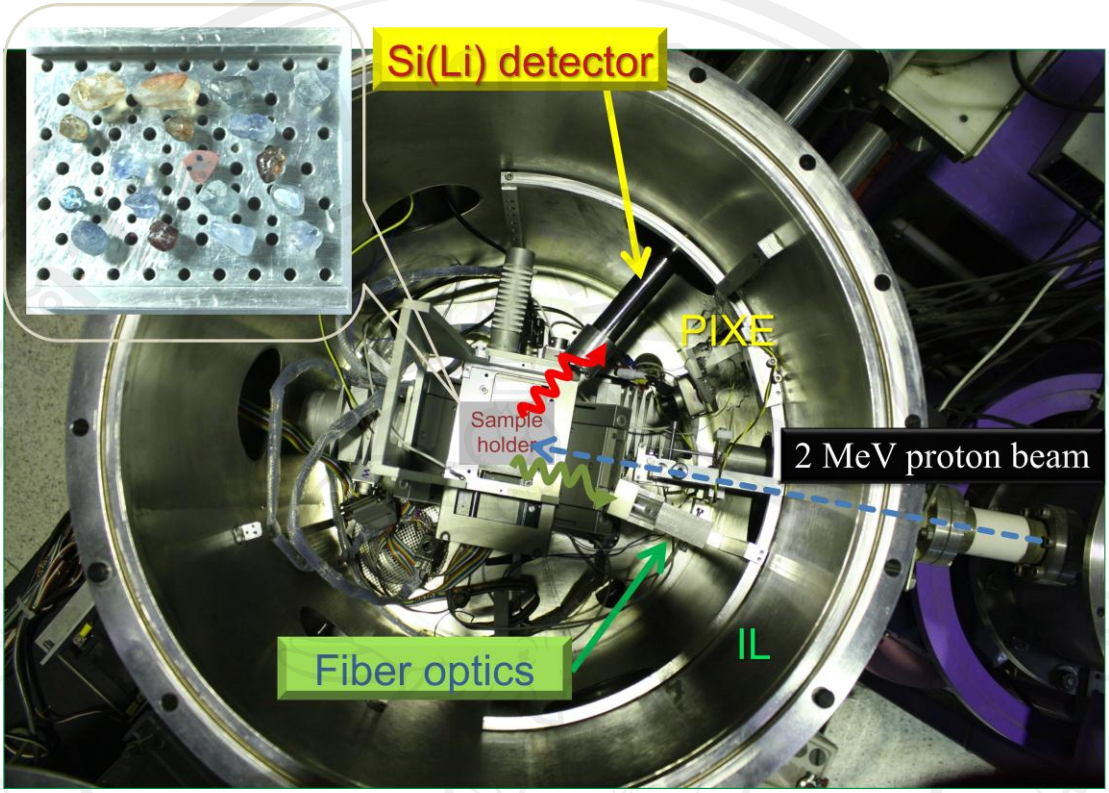

Figure 2.15. The equipment set up inside the analysis chamber.

In addition, the beam current at the sample was kept below 10 nA. Base pressure in the vacuum chamber had to below 1×10^{-5} torr. Each measurement was taken for approximately 900 seconds or below in the real-measuring time that eliminated the dead time.

2.3.4 Data accumulation, acquisition of IL technique

Also seen in Figure 2.15, there is a fiber optic light guide inside the analysis chamber which placed at about 200^{o} to the beam direction with closing distance to the sample by also avoiding the ion beam trajectory. The end of the fiber is placed close to corundum sample for guiding the luminescent light out of the chamber to the

outside spectrometer (Ocean Optics S2000 spectrometer). Inside this device, there is a reflection grating of 600 lines per 1 mm width for resolving the income light and distribute them to the 2,048 pixels on the CCD. Then, the alternated voltage in CCD is sent to the analog to digital convertor (ADC1000) module which connects to the socket in a personal computer beside the analysis chamber. After this, a personal computer was installed the OOIBase32 software (Ocean Optics, Inc, 1999) to accumulate the light spectrum. More details are stated by Krua-in (2006). The measurement in each investigation usually regards on the luminescence characteristic in the materials in the range of 200 – 800 nm for 500 – 3,000 ms. Prior to the experiment, the channel number and wavelength calibration must be done so that the HG – 1 mercury argon standard light source is used for calibrated as shown the result in Kamwanna (2008).

The IL system set up is shown in Figure 2.16. For qualitative analysis, the emission spectra of IL are compared with the absorption spectra of UV-Vis-NIR spectra directly. This explanation can be used for identifying the ion-induced luminescence mechanism, leading to a determination of the color differences with a conventional method.

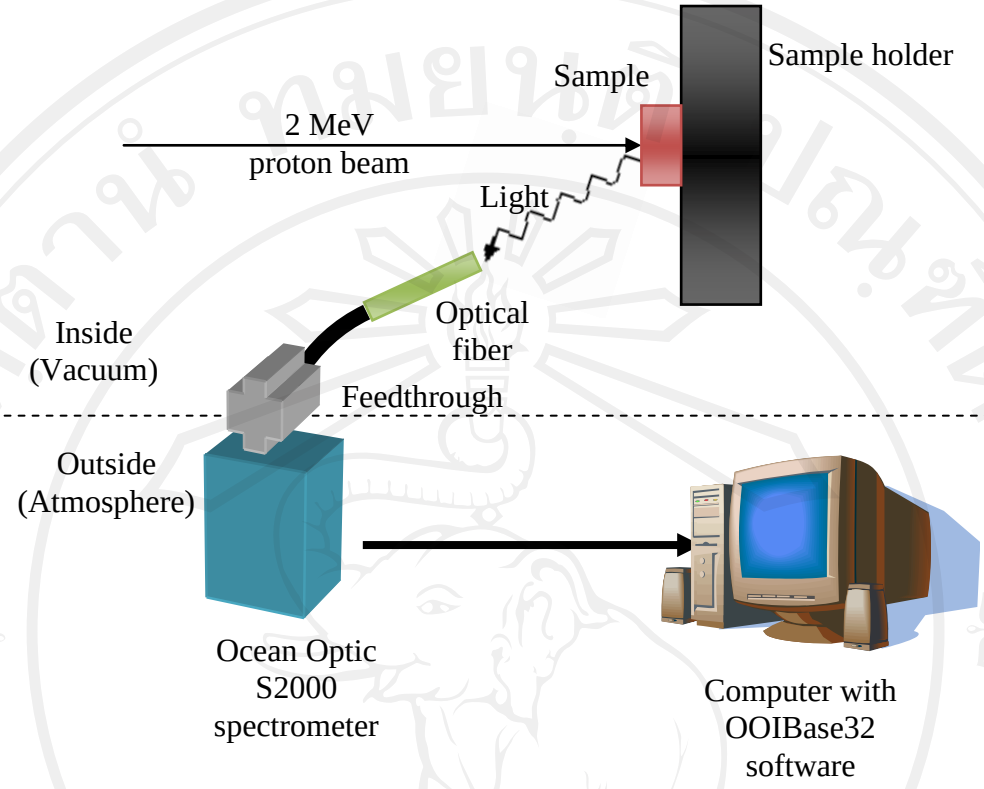

Figure 2.16. The diagram of IL accumulation system.